


# Multi-segmented nanowires for vortex magnetic domain wall racetrack memory

M Al Bahri, M Al Hinaai, and T Al Harthy
**Citation:**Chin. Phys. B, 2023, 32 (**12**): 127508. DOI: 10.1088/1674-1056/acca0a
Journal homepage: http://cpb.iphy.ac.cn; http://iopscience.iop.org/cpb

**What follows is a list of articles you may be interested in**

---

## In-plane spin excitation of skyrmion bags

Shuang Li(李爽), Ke-Xin Li(李可欣), Zhao-Hua Liu(刘照华), Qi-Yuan Zhu(朱起源), Chen-Bo Zhao(赵晨博), Hu Zhang(张虎), Xing-Qiang Shi(石兴强), Jiang-Long Wang(王江龙), Rui-Ning Wang(王瑞宁), Ru-Qian Lian(连如乾), Peng-Lai Gong(巩朋来), and Chen-Dong Jin(金晨东)
Chin. Phys. B, 2023, 32 (**11**): 117503. DOI: 10.1088/1674-1056/acd327

## Magnonic band-pass and band-stop filters with structurally modulated waveguides

Lai-He Feng(冯来和), Mang-Yuan Ma(马莽原), Zhi-Hua Liu(刘智华), Kai-Le Xie(解凯乐), and Fu-Sheng Ma(马付胜)
Chin. Phys. B, 2023, 32 (**6**): 067503. DOI: 10.1088/1674-1056/ac8afb

## Gate-voltage control of alternating-current-driven skyrmion propagation in ferromagnetic nanotrack devices

Xin-Yi Cai(蔡心怡), Zhi-Hua Chen(陈志华), Hang-Xiao Yang(杨航霄), Xin-Yan He(何鑫岩), Zhen-Zhen Chen(陈珍珍), Ming-Min Zhu(朱明敏), Yang Qiu(邱阳), Guo-Liang Yu(郁国良), and Hao-Miao Zhou(周浩淼)
Chin. Phys. B, 2023, 32 (**6**): 067502. DOI: 10.1088/1674-1056/acb420

## Micromagnetic study of magnetization reversal in inhomogeneous permanent magnets

Zhi Yang(杨质), Yuanyuan Chen(陈源源), Weiqiang Liu(刘卫强), Yuqing Li(李玉卿), Liying Cong(丛利颖), Qiong Wu(吴琼), Hongguo Zhang(张红国), Qingmei Lu(路清梅), Dongtao Zhang(张东涛), and Ming Yue(岳明)
Chin. Phys. B, 2023, 32 (**4**): 047504. DOI: 10.1088/1674-1056/ac9359

## Skyrmion-based logic gates controlled by electric currents in synthetic antiferromagnet

Linlin Li(李林霖), Jia Luo(罗佳), Jing Xia(夏静), Yan Zhou(周艳), Xiaoxi Liu(刘小晰), and Guoping Zhao(赵国平)
Chin. Phys. B, 2023, 32 (**1**): 017506. DOI: 10.1088/1674-1056/ac9b01

---

# Multi-segmented nanowires for vortex magnetic domain wall racetrack memory

M Al Bahri[†], M Al Hinaai, and T Al Harthy

*Department of Basic Sciences, A'Sharqiyah University, Post Box* 42, *PC* 400, *Ibra, Oman*

(Received 10 January 2023; revised manuscript received 1 March 2023; accepted manuscript online 4 April 2023)

A vortex domain wall's (VW) magnetic racetrack memory's high performance depends on VW structural stability, high speed, low power consumption and high storage density. In this study, these critical parameters were investigated in magnetic multi-segmented nanowires using micromagnetic simulation. Thus, an offset magnetic nanowire with a junction at the center was proposed for this purpose. This junction was implemented by shifting one portion of the magnetic nanowire horizontally in the $x$-direction ($l$) and vertically ($d$) in the $y$-direction. The VW structure became stable by manipulating magnetic properties, such as magnetic saturation ($M_s$) and magnetic anisotropy energy ($K_u$). In this case, increasing the values of $M_s \geq 800$ kA/m keeps the VW structure stable during its dynamics and pinning and depinning in offset nanowires, which contributes to maintenance of the storage memory's lifetime for a longer period. It was also found that the VW moved with a speed of 500 m/s, which is desirable for VW racetrack memory devices. Moreover, it was revealed that the VW velocity could be controlled by adjusting the offset area dimensions ($l$ and $d$), which helps to drive the VW by using low current densities and reducing the thermal-magnetic spin fluctuations. Further, the depinning current density of the VW ($J_d$) over the offset area increases as $d$ increases and $l$ decreases. In addition, magnetic properties, such as the $M_s$ and $K_u$, can affect the depinning process of the VW through the offset area. For high storage density, magnetic nanowires (multi-segmented) with four junctions were designed. In total, six states were found with high VW stability, which means three bits per cell. Herein, we observed that the depinning current density ($J_d$) for moving the VW from one state to another was highly influenced by the offset area geometry ($l$ and $d$) and the material's magnetic properties, such as the $M_s$ and $K_u$.

**Keywords:** micromagnetic simulation, vortex domain wall racetrack memory, multi-segmented magnetic nanowire, spin transfer torque

**PACS:** 75.75.Fk **DOI:** 10.1088/1674-1056/acca0a

## 1. Introduction

Future storage memory novel properties, such as low power consumption, high speed for reading and writing of the stored information, storage of multi-bit per cell and spin-transfer torque driving have been the subject of recent developments.[1–7] Racetrack memory is one application of future storage memory.[8,9] Thus, several studies have focused on studying the current induced domain wall (DW) motion to improve critical issues like the DW's heat fluctuation.[10,11] Other studies have examined the DW speed and how to improve the DW speed reduction related to various parameters, such as the Walker field.[12–15] However, other researchers have concentrated on using different ways to trap the DW at certain positions within devices.[16–23] Triangular notches are the most common DW trapping methods, although this has some limitations: for example, their shape facilitates the VW structural transformation. However, the notching process is complex and costly, especially for devices with ten-nanometer widths and nonuniform pinning.[24–28] The manipulation of driven DW using spin currents is the key for future spintronics storage devices. Herein, the challenge is maintaining the DW's structure during the dynamics and pinning process for the construction of racetrack memory, especially with magnetic vortex racetrack memory.[29–32] In this work, we propose a VW storage memory using offset magnetic nanowires. The proposed scheme consists of two nanowire segments with an offset area in the center, as shown in Fig. 1(a). Using this offset device with nanoscale dimensions will help to lower the power consumption. Furthermore, the design of the offset area as the overlapping between two nanowire edges will help to pin the VW precisely by adjusting the length of the offset area ($l$) and its depth ($d$). Moreover, the offset area is free of the sharp edges in its center. This helps to protect the VW structure from transformations during its pinning and depinning process, which extends the memory life. In addition, with the offset nanowire, the VW speed could be controlled by altering the geometry of the offset area, such as $l$ and $d$. Unlike the spin valve, the offset device can play a role in storing more than one bit per cell by increasing the number of junctions in one cell, as shown in Fig. 1(b). In this work, with this proposed scheme, the structural stability of the VW during the dynamics and pinning process is examined due to magnetic properties such as saturation magnetization ($M_s$). A study of the VW speed is subsequently carried out based on the current density and the geometry of the offset area.

Finally, a multi-segmented magnetic nanowire is designed to increase the storage density with four junctions to

[†]Corresponding author. E-mail: mohammed.albahri@asu.edu.om

© 2023 Chinese Physical Society and IOP Publishing Ltd 

obtain six states per cell (three bits), as shown in Fig. 1(b).

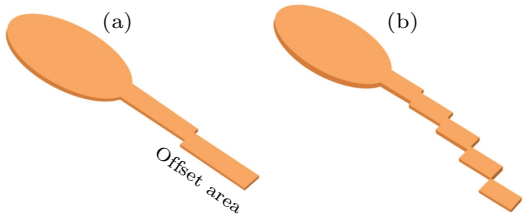



**Fig. 1.** (a) The offset magnetic nanowire. (b) The multi-segmented magnetic nanowire for high storage density.

## 2. Modeling

The dynamics of VWs with tail to tail ( TT) configurations in offset nanowire are carried out using a framework of OOMMF codes at 0 K[33] based on the Landau–Liftshitz–Gilbert (LLG) equation with a spin-transfer torque (STT) term, according to the Zhang and Li model[34,35]

$$\frac{\mathrm{d}\boldsymbol{m}}{\mathrm{d}t} = -\gamma \boldsymbol{m} \times \boldsymbol{H}_{\mathrm{eff}} + \alpha \boldsymbol{m} \times \frac{\mathrm{d}\boldsymbol{m}}{\mathrm{d}t} + (\boldsymbol{u}\cdot\nabla)\boldsymbol{m} + \beta \boldsymbol{m} \times (\boldsymbol{u}\cdot\nabla)\boldsymbol{m}. \quad (1)$$

We consider the fact that the magnetic properties are used for in-plane magnetic materials, such as permalloy, $CO_{90}Fe_{10}$ and $Ni_{81}Fe_{19}$.[36] The damping coefficient $\alpha$ is fixed to 0.01, the nonadiabatic constant $\beta$ is chosen as 0.04 for all simulations and the exchange stiffness is $A = 1.3 \times 10^{-11}$ J/m[37] and $\boldsymbol{u} = (gP\mu_{\mathrm{B}}/(2eM_{\mathrm{s}}))J$.[38]

Offset magnetic nanowires with the geometries of $L$(2000 nm)×$w$(200 nm)×$t$(30 nm) are considered in this study. These dimensions are chosen due to the availability of the VW depending on nanowire sizes.[39,40] A cubic cell size (mesh size) of $5 \times 5 \times 5$ nm$^3$ is selected, and is sufficiently smaller than the exchange length (≈ 5.3 nm).

At the nanowire center, an offset junction is created by shifting one part vertically in the $y$-direction with vertical length ($d$) and horizontal length ($l$) in the $x$-direction. Figure 2(a) shows the initial state with the dimensions of the offset magnetic nanowire.

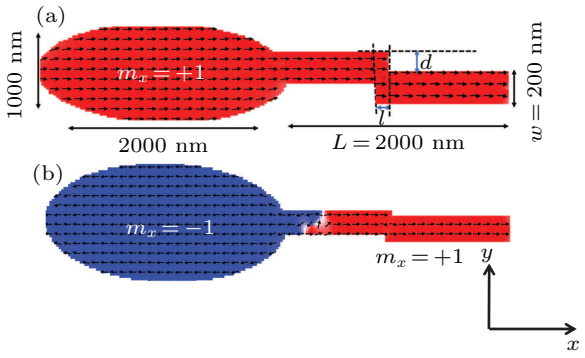



**Fig. 2.** (a) An OOMMF image of magnetic offset magnetic nanowire dimensions with an initial state where all spins are configurated to the positive $x$-direction ($m_x = +1$). (b) An OOMMF image of VW motion in offset nanowire under a value of current density ($J = 2 \times 10^{11}$ A/m$^2$).

The offset nanowire is connected with a nucleation pad with dimensions of length 2000 nm and width 1000 nm. Initially, the current density is applied in the positive $x$-direction to saturate the magnetization in this direction (red color), as in Fig. 2(a). Then, the current density with a value of $2 \times 10^{11}$ A/m$^2$ is used to create VWs with tail to tail magnetization at the nucleation pad, and one of them is propagated in the offset magnetic nanowire [Fig. 2(b)].

## 3. Results and discussion

Different parameters, such as the high stability, fast access, and large density of VW racetrack magnetic storage devices, have been investigated in this study using offset magnetic nanowires.

### 3.1. VW structural stability

One parameter for the construction of a stable VW magnetic racetrack memory is the VW structural stability during its dynamics in magnetic nanowires.[41] Thus, the effects of magnetic properties, such as $M_{\mathrm{s}}$ and offset area dimensions, on VW structural stability before reaching the offset area are studied first. Simulations are formed using offset nanowires with fixed $l = 50$ nm and varying $d$ (50 nm, 100 nm, 150 nm). It is found that by increasing the values of the offset area depth ($d$), the VW loses its structural stability and converts to TW early during its dynamics before reaching the offset area. Thus, increasing the values of $M_{\mathrm{s}}$ helps to maintain the VW structure. With the magnetic nanowire with offset area ($l = 50$ nm and $d = 50$ nm), it is seen that the VW has less structural stability with $M_{\mathrm{s}} \leq 700$ kA/m in its dynamics toward the offset area and it converts to a transverse domain wall (TW). However, the VW becomes stable in its structure with $M_{\mathrm{s}}$ values of $\geq 800$ kA/m and no structural changes are observed. For example, with an $M_{\mathrm{s}}$ of 500 kA/m, the VW converted to TW after 1 ns of starting its motion, as shown in Fig. 3(b), while its structure is stable for 2.5 ns with $M_{\mathrm{s}}$ of 600 kA/m, as illustrated in Fig. 3(c). As the $M_{\mathrm{s}}$ is increased to 700 kA/m [Fig. 3(d)], it can be seen that the VW maintains its structure for 6.5 ns until it reaches the offset area, before transforming to a TW within the constricted region. However, the VW has high stability in its structure with $M_{\mathrm{s}} \geq 800$ kA/m and has pinned at the offset area as a VW, as illustrated in Fig. 3(e). To better understand how the $M_{\mathrm{s}}$ affects VW structural stability in offset nanowire ($d = 50$ nm and $l = 50$ nm), Fig. 3(f) presents the plot of normalized magnetization in the $x$-direction ($m_x$) versus time for different values of $M_{\mathrm{s}}$. The circled dashed area indicates the time of switching of the VW to TW during the VW dynamics (i.e., $M_{\mathrm{s}} = 500$ kA/m and 600 kA/m). In contrast, by increasing the $M_{\mathrm{s}}$ to values of $\geq 700$ kA/m, the VW becomes more stable and its graph becomes smooth, without any indication of the transformation type [$M_{\mathrm{s}} = 700$ kA/m and 800 kA/m].

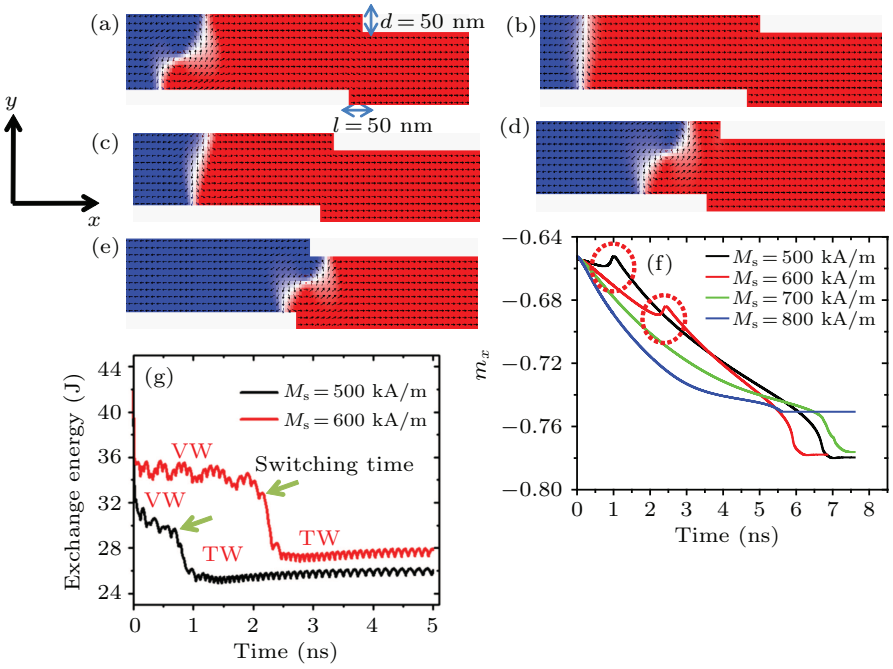



**Fig. 3.** (a) An OOMMF image of VW dynamics in offset nanowire with a constricted area of ($l = 50$ nm and $d = 50$ nm). (b)–(c) OOMMF images of a VW switching to a TW with values of $M_s \leq 700$ kA/m. (d)–(e) OOMMF images of a VW that is stable in its structure and that pins at the offset area as a VW with values of $M_s \geq 800$ kA/m. (f) The time dependence of $m_x$ for different values of $M_s$ in offset nanowire with a constricted area of ($l = 50$ nm and $d = 50$ nm). (g) The plot of exchange energy versus time for $M_s = 500$ kA/m and 600 kA/m.

A VW transformation results from competition between exchange energy, which keeps the magnetic field surrounding the core and the easy axes' energy, which keeps the DW magnetization on the easy axes as a TW. To understand the effect of $M_s$ on VW transformation, exchange energy is plotted against time for two values of $M_s$, as shown in Fig. 3(g). It is found that the VW has higher exchange energy when increasing the $M_s$. As a result, there is an improvement in the VW structure stability. For more confidence that the VW has more structural stability with increasing $M_s$ values, more investigations are carried out using offset nanowire with area dimensions of ($l = 50$ nm and $d = 100$ nm); it is seen that the VW changes its type to TW, as observed for the nanowire with dimensions of ($l = 50$ nm and $d = 50$ nm) for $M_s = 500$ kA/m and 600 kA/m [Figs. 4(b) and 4(c)]. However, for $M_s = 700$ kA/m, the VW converts after 3.5 ns to TW before reaching the offset area, as shown in Fig. 4(d). More structural stability is observed with 700 kA/m$< M_s <$ 900 kA/m, where the VW converts to TW at the offset area [Fig. 4(e)]. To maintain the VW structure in the ($l = 50$ nm and $d = 100$ nm) magnetic nanowire, $M_s$ values should reach up to 900 kA/m or higher ($M_s \geq 900$ kA/m), as evidenced by the plot of the $m_x$ versus time in Fig. 4(f).

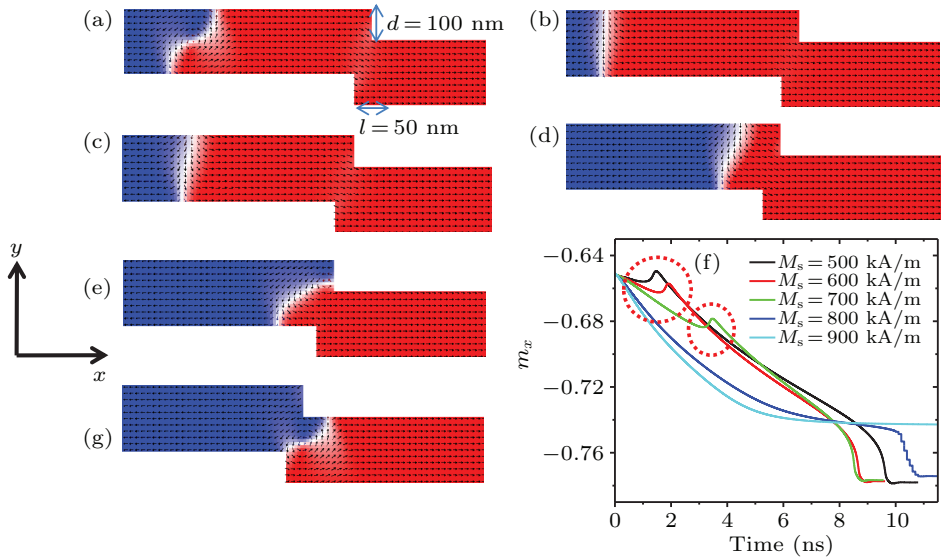



**Fig. 4.** (a) An OOMMF image of VW dynamics in offset nanowire with a constricted area of ($l = 50$ nm and $d = 100$ nm). (b)–(d) OOMMF images of the VW converting to TW with values of $M_s \leq 700$ kA/m. (e) An OOMMF image of the VW transforming to TW at an offset area with 700 kA/m$< M_s <$ 900 kA/m. (g) The VW becomes stable and pins at the offset area ($M_s \geq 900$ kA/m). (f) A plot of $m_x$ as a function of time in offset nanowire with a constricted area of ($l = 50$ nm and $d = 100$ nm).

When increasing the depth of the offset area to $d = 150$ nm, the VW becomes less stable and needs to use values of $M_s \geq 1000$ kA/m to maintain its structure until it is trapped by the offset area. Figures 5(b)–5(d) show the VW transformation under the values of $M_s \leq 700$ kA/m with the same VW transformation time as in the nanowires with ($l = 50$ nm and $d = 50$ nm) and ($l = 50$ nm and $d = 100$ nm). However, in this nanowire of offset dimensions ($l = 50$ nm and $d = 150$ nm), the VW remains stable in its structure until it is pinned at the offset area with only $M_s$ values of 1000 kA/m and higher ($M_s \geq 1000$ kA/m), as illustrated in Fig. 5(f). Figure 5(g) shows the $m_x$ versus time for different values of $M_s$. As can be seen, the VW switching varies depending on the $M_s$ values. However, with the $M_s$ of 1000 kA/m, the curve actually becomes smooth without any sign of VW switching.

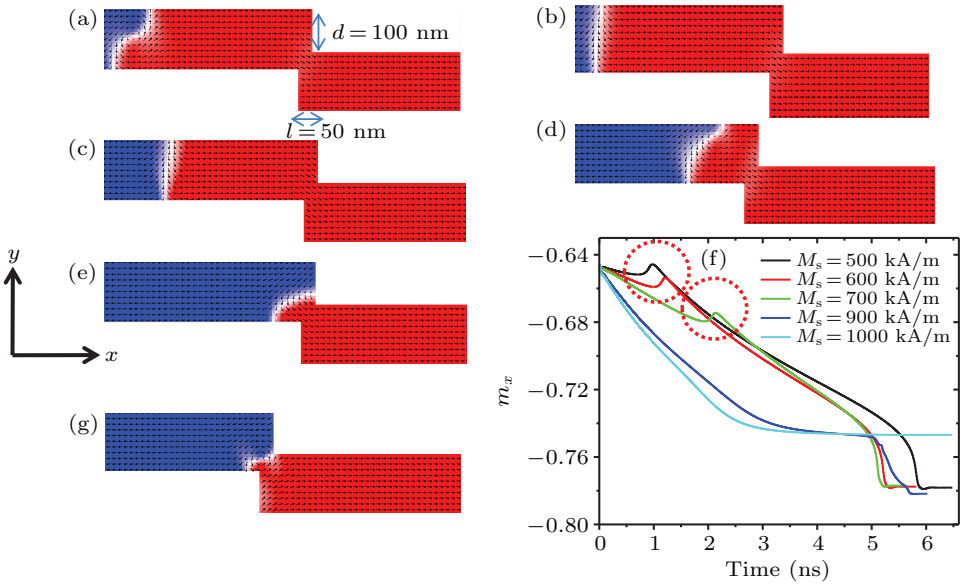



**Fig. 5.** (a) An OOMMF image of VW dynamics in offset nanowire with an offset area of ($l = 50$ nm and $d = 150$ nm). (b)–(d) OOMMF images of the VW converting to TW with values of $M_s \leq 700$ kA/m. (e) The VW transforms to TW at the offset area with 700 kA/m$< M_s <$ 1000 kA/m. (g) The VW becomes stable and pins at the offset area ($M_s \geq 1000$ kA/m). (f) A plot of $m_x$ as a function of time in offset nanowire with an offset area of ($l = 50$ nm and $d = 150$ nm).

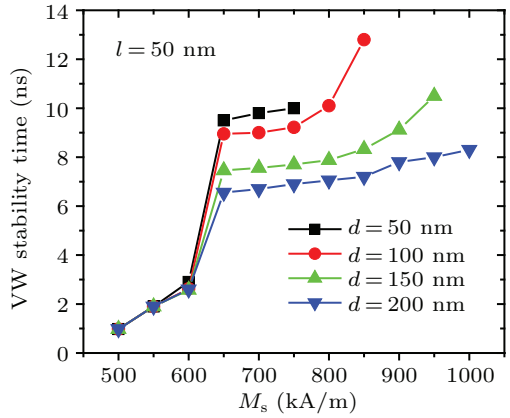



**Fig. 6.** The VW structure stability time dependence of $M_s$ in different nanowire structures of offset areas.

For a better understanding of the effect of increasing $d$ on the VW structural stability time, the VW structure stability time is plotted against $M_s$ for several nanowire structures [Fig. 6]. It can be observed that there is no effect of any variations in $d$ on VW structural stability time for values of $M_s \leq 600$ kA/m, and the transformation takes place before the VW reaches the offset area at the same time in different nanowires. However, the effect of $d$ on VW switching becomes obvious when the VW reaches the offset area for $M_s \geq 700$ kA/m. Herein, it is found that the VW structural stability time decreases when increasing $d$ for the same $M_s$ value. For an instant, the VW switches to TW with $M_s$ of 800 kA/m after 10 ns in magnetic nanowire with $d = 100$ nm, while it undergoes transformation after 8 ns and 6 ns in nanowire with offset areas of $d = 150$ nm and 200 nm, respectively. Moreover, it is noted from the graph that an increasing $d$ leads to a linear relationship between the VW stability time and $M_s$.

### 3.2. VW speed

The effect of increasing $d$ on VW stability time leads to the investigation of the effect of the variation of $d$ on VW motion. Thus, the influence of increasing $d$ on VW speed is studied. Here, the $M_s$ of 1100 kA/m is used to maintain the VW structure during its motion until it gets pinned at the offset area. Figure 7(a) shows the plot of VW velocity dependence on current density in nanowires with different values of $d$. It is noted that the VW velocity changes linearly with current density and this agrees with the equation

$$v = \frac{gP\beta\mu_B}{2e\alpha M_s} J, \tag{2}$$

where $J$ is the current density, $g$ is the Lande factor, $P$ is the spin polarization, $e$ is the carrier charge, $\mu_B$ is the Bohr mag-

neton, $\beta$ is the non-adiabatic parameter and $\alpha$ is the Gilbert damping factor.[38]

In addition, it is found that VW dynamics increase by increasing the offset area geometry $d$ due to the decrease in the easy axis's energy in positive $x$-axes, which means that the VW magnetization switches from the positive $x$-axes direction to the negative will be faster and, therefore, the VW moves faster. For example, with a current density value of $6 \times 10^{11}$ A/m$^2$, the VW moves with the speed of 250 m/s in a nanowire with an offset area of $d = 50$ nm, while it moves with 280 m/s in the offset nanowire with $d = 100$ nm and with 310 m/s in the nanowire with $d = 150$ nm.

Figures 7(b)–7(e) show snapshot images of the VW at different positions in nanowires of $d$ (50 nm, 100 nm, 150 nm and 200 nm) under a driven current density of $1.2 \times 10^{12}$ A/m$^2$ at the same time of 1.65 ns from the start of its motion. It is observed that by increasing $d$, the VW has crossed farther distances at this time (1.65 ns). Thus, the VW is closer to the offset area in the nanowire with $d$ of 200 nm [Fig. 7(e)]. For future VW memory, the VW should move with a speed of 100 m/s and higher. Using offset nanowire, we achieve the result that the VW moves with a speed of 500 m/s, which is desirable for fast writing and reading of stored information. Meanwhile, in the literature, they have only achieved 200 m/s.[32] More efficient results for increasing the VW velocity by manipulating the offset geometry are obtained via reduction of the VW thermal fluctuations by driving VWs at low current densities.

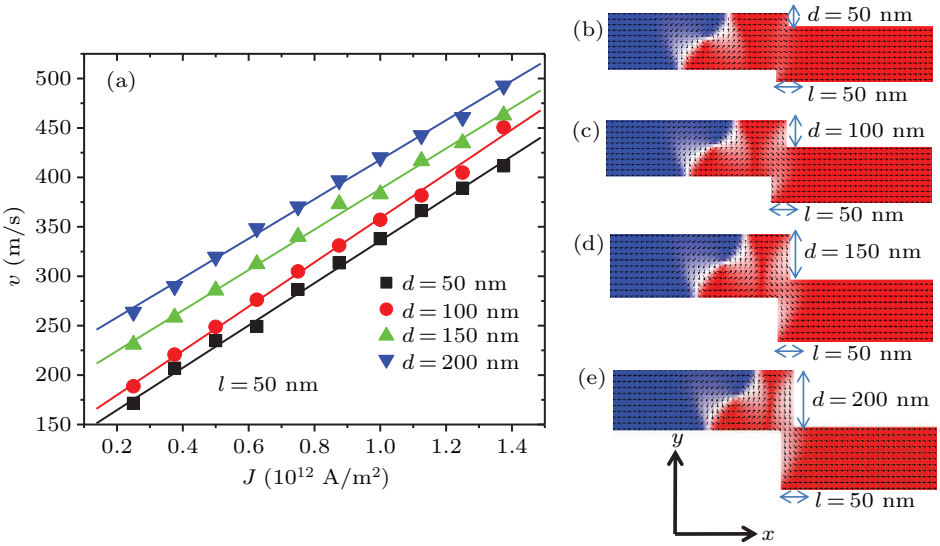



**Fig. 7.** (a) The plot of VW velocity as a function of current density in offset nanowire with different values of $d$. OOMMF images of the VW position at the time of 1.65 ns and in the offset nanowire with $l = 50$ nm and (b) $d = 50$ nm, (c) 100 nm, (d) 150 nm and (e) 200 nm.

### 3.3. VW pining at offset area

For high performance of the VW magnetic racetrack memory, the VW should be pinned at the offset area. This pinning strength depends on the offset area dimensions ($l$ and $d$) and the development of magnetic properties, such $M_s$ and $K_u$. Thus, the depinning current density ($J_d$) over the offset area geometry ($l$ and $d$) is investigated. It is found that the depinning current density increases linearly with $d$ [Fig. 8(a)], while it decreases with increasing $l$, as shown in Fig. 8(b).

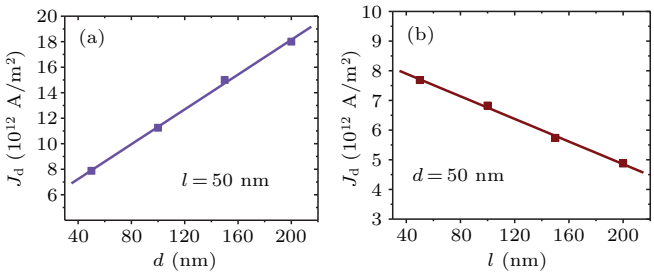



**Fig. 8.** VW depinning current density versus (a) $d$ with fixed $l$ to 50 nm and (b) $l$ with fixed $d$ to 50 nm. The magnetic properties of the investigated material are $K_u = 0.5 \times 10^5$ J/m$^3$ and $M_s = 1100$ kA·m.

Furthermore, depinning current density ($J_d$) values based on $M_s$ and $K_u$ are investigated using different offset area dimension values ($l$ and $d$). Figure 9 shows the graph of $J_d$ versus $d$ for different values of $M_s$ and $K_u$. In these graphs, it is obvious that $J_d$ increases when the $M_s$ or $K_u$ values increase. It is worth noting that $J_d$ has linear behavior with $d$ for different values of $M_s$ and $K_u$, which would add critical improvements for high VW storage memory with a long lifetime.

For example, in the nanowire with offset area dimensions of ($l = 50$ nm and $d = 100$ nm), $J_d$ is $7.5 \times 10^{12}$ A/m$^2$ for the $M_s$ of 1100 kA/m, while it is $11 \times 10^{12}$ A/m$^2$ and $15 \times 10^{12}$ A/m$^2$ for the $M_s$ of 1150 kA/m and 1200 kA/m, respectively [Fig. 9(a)]. The effects of $K_u$ on VW pinning with varying $d$ are the same as for $M_s$. The results are plotted in the graph of $J_d$ versus $K_u$, as shown in Fig. 9(b). To get a better understanding of the effects of $l$ on $J_d$ (the offset nanowire junctions), nanowires are proposed with fixed values of $d$ (50 nm) and the values of $l$ are varied by 50 nm. Figure 9(c) shows the plot of $J_d$ dependence on $l$ for different values of $M_s$, showing that the $J_d$ decreases with increasing $l$ values and the same

results are observed with different values of $K_u$ [Fig. 9(d)]. These results have confirmed that the pinning potential of the offset nanowire has increased by improving the values of $M_s$ and $K_u$.

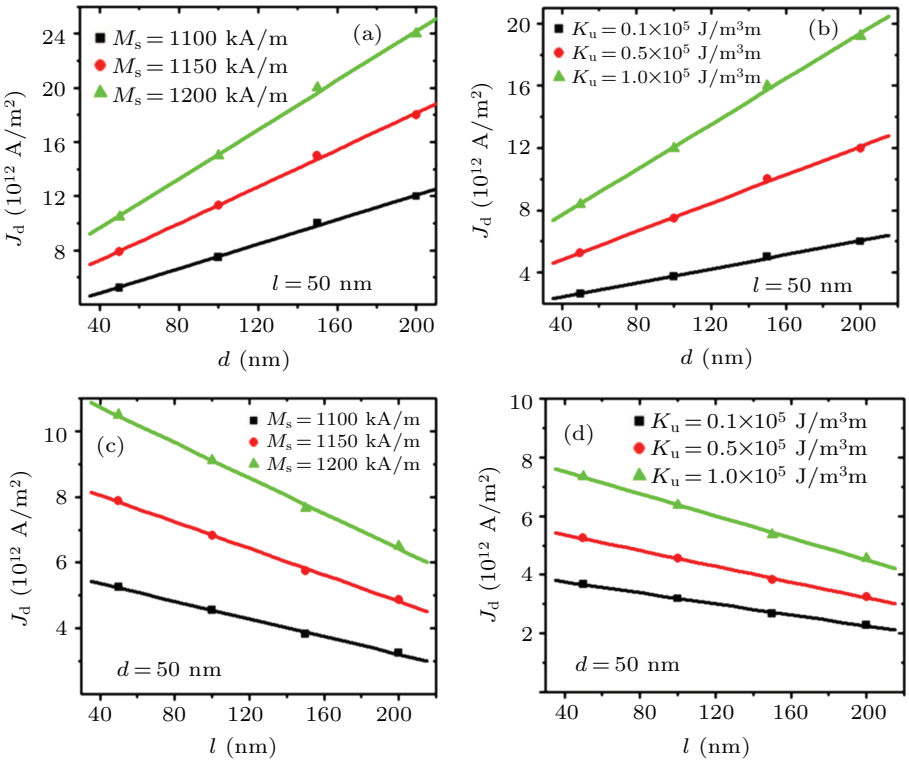



**Fig. 9.** (a) The plot of $J_d$ as a function of (a) $d$ for three values of $M_s$, (b) $d$ for three values of $K_u$, (c) $l$ for three values of $M_s$ and ($d$) $l$ for three values of $K_u$.

### 3.4. VW multi-bit per cell

A critical parameter for future VW storage memory is to increase the storage density to more than one bit per cell. For this implementation, the offset nanowire is designed with four junctions by increasing the values of $d$ from left to right and keeping $l$ fixed (50 nm). To maintain the VW structural stability, the $M_s$ is kept to 1100 kA/m. The possibility of storing six states using the offset nanowire with four junctions is also investigated. It is noted from Fig. 10 that six states are obtained, and Fig. 10(a). shows a plot of the $m_x$ dependence of current density for the six states. Figure 10(b) shows the first state where all spins pointed to the positive $x$-direction while increasing the current density to $1 \times 10^{12}$ A/m$^2$; the VW is created and moves to become pinned at the first junction to represent the second state [Fig. 10(c)]. Once the current density is increased to reach the value of $2.5 \times 10^{12}$ A/m$^2$, the VW leaves the first junction and moves to the second one and gets trapped there. This represents the third state and so on, until the VW moves to the end of the nanowire, as shown in Fig. 10(g).

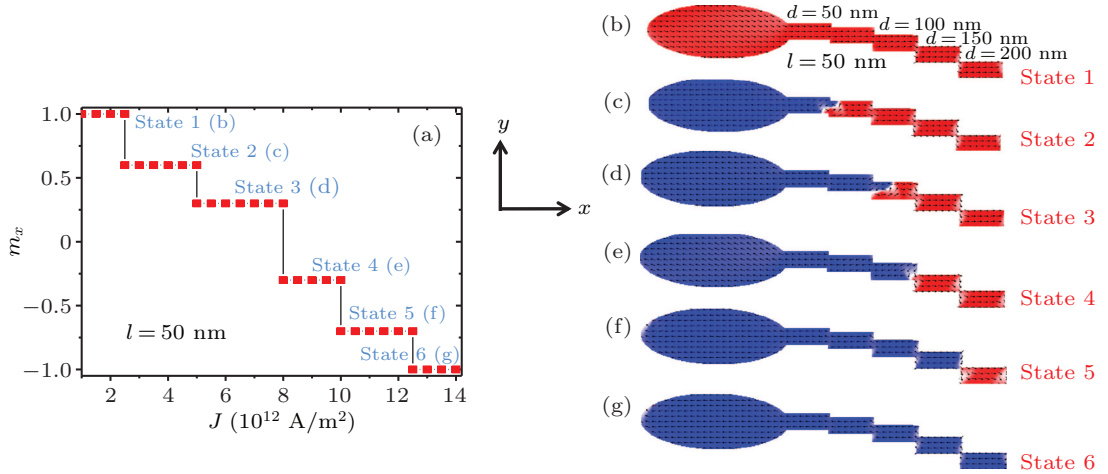



**Fig. 10.** The six states of multi-segmented magnetic nanowires with $L = 1000$ nm, $w = 200$ nm and $t = 30$ nm. The magnetic properties are $M_s = 1100$ kA/m and $0.5 \times 10^5$ J/m$^3$. (b) The first state and (c) the second state, where the VW is pinned at the first junction ($d = 50$ nm). (d) The third state, where the VW is pinned at the second junction ($d = 100$ nm). (e) The fourth state, where the is VW pinned at the third junction ($d = 150$ nm). (f) The fifth state, where the VW is pinned at the fourth junction ($d = 200$ nm), and (g) the sixth state, where the VW moves to the end of the nanowire.

## 4. Conclusion

In summary, several properties of VW magnetic racetrack memory were investigated using offset magnetic nanowires for future high speed, high density and long lifetime storage memory. It was found that VW transformation could be controlled by increasing the $M_s$. For $M_s$ values of $\geq$ 800 kA/m, the VW structure was stable during its dynamics and depinning process, which helps to maintain the long lifetime of the storage devices. Using offset magnetic nanowires, a VW maximum speed of 500 m/s has been achieved to implement fast access memories. We found that the VW speed could be controlled by adjusting the offset area dimensions ($l$ and $d$) and the driven current density. Six stable states were achieved using multi-segmented nanowires with four junctions. The VW pinning through the junction depends on the junction sizes ($l$ and $d$) and magnetic properties ($M_s$ and $K_u$). It was observed that $J_d$ increases with increasing $d$ or magnetic properties and decreases with increasing $l$ or magnetic properties.

## References


[1] Berger L 1996 *Phys. Rev. B* **54** 9353
[2] Shinjo T, Okuno T, Hassdorf R, Shigeto K and Ono T 2000 *Science* **289** 930
[3] Beach G, Knutson C, Nistor C, Tsoi M and Erskine L 2006 *Phys. Rev. Lett.* **97** 057203
[4] Kent A D and Worledge D C 2015 *Nat. Nanotech.* **10** 187
[5] Grollier J, Boulenc P, Cros V, Hamzić A, Vaurès A, Fert A and Faini G 2003 *Appl. Phys. Lett.* **83** 509
[6] Gupta S, Sbiaa R, Al Bahri M, Ghosh A, Piramanayagam S N, Ranjbar M and Akerman J 2018 *J. Phys. D: Appl. Phys.* **51** 465002
[7] Hayashi M, Thomas L, Moriya R, Rettner C and Parkin S S P 2008 *Science* **320** 209
[8] Allwood D A, Xiong G, Faulkner C, Atkinson D, Petit D, Cowburn R P 2005 *Science* **309** 1688
[9] Gaidis M C and Thomas L 2013 *Nanoscale Semiconductor Memories: Technology and Applications* **190** 229
[10] Yamanouchi M and Leda J 2008 *Science* **317** 1726
[11] Al Bahri M 2022 *J. Magn. Magnet. Mater.* **543** 168611
[12] Brandão J, Novak R L, Lozano H, Soledade P R, Mello A, Garcia F and Sampaio L C 2014 *J. Appl. Phys.* **116** 193902
[13] Mohanan V P and Kumar P 2017 *J. Magn. Magnet. Mater.* **422** 419
[14] Wilhelm E S, McGrouther D, Heyne L, Bisig A and Kläui 2009 *Appl. Phys. Lett.* **95** 252501
[15] Wieser R, Vedmedenko E Y, Weinberger P and Wiesendanger R 2010 *Phys. Rev. B* **82** 144430
[16] Jin T, Kumar D, Gan W, Ranjbar M, Luo F, Sbiaa R, Liu X, Lew W S and Piramanayagam S N 2018 *Phys. Status Solidi - Rapid Research Letters* **12** 1800197
[17] Hayashi M, Thomas L, Rettner C, Moriya R, Jiang X and Parkin S S P 2006 *Phys. Rev. Lett.* **97** 207205
[18] Komine T, Murakami H, Nagayama T and Sugita R 2008 *IEEE Transactions on Magnetics* **44** 2516
[19] Kunz A and Priem J D 2010 *IEEE Transactions on Magnetics* **46** 1559
[20] Rahm M, Biberger J, Umansky V and Weiss D 2003 *J. Appl. Phys.* **93** 7429
[21] Al Bahri M and Sbiaa R 2016 *Scientific Reports* **6** 28590
[22] Sbiaa R and Al Bahri M 2016 *J. Magn. Magnet. Mater.* **411** 113
[23] Al Bahri M, Borie B, Jin T L, Sbiaa R, Kläui M and Piramanayagam S N 2019 *Phys. Rev. Applied* **10** 024023
[24] Noh S J, Miyamoto Y, Okuda M, Hayashi N and Keun Y 2012 *J. Appl. Phys.* **111** 07D123
[25] Ho L D A, Tran M T, Cao X H, Dao V A, Ngo D T and Hoang D Q 2018 *RSC Advances* **8** 14539
[26] Paixão E L M, Toscano D, Gomes J C S, Monteiro M G, Sato F, Leonel S A and Coura P Z 2018 *J. Magn. Magnet. Mater.* **451** 639
[27] Bogart L K, Atkinson D, O'Shea K, McGrouther D and McVitie S 2009 *Phys. Rev. B* **79** 054414
[28] Eastwood D S, Bogart L K and Atkinson D 2010 *Acta Physica Polonica A* **118** 719
[29] McMichael R D and Donahue M J 1997 *IEEE Transactions on Magnetics* **33** 4167
[30] Yershov K V, Kravchuk V P, Sheka D D and Gaididei Y 2014 *J. Appl. Phys.* **117** 083908
[31] Streubel R, Kronast F, Reiche C F, Mühl T, Wolter A, Schmidt O G and Makarov D 2016 *Appl. Phys. Lett.* **108** 042407
[32] Geng L D and Jin Y M 2017 *J. Magn. Magnet. Mater.* **423** 84
[33] Zhu W, Liao J, Zhang Z, Ma B, Jin Q, Liu, Huang Z, Hu X, Ding A, Wu J, and Xu Y 2012 *Appl. Phys. Lett.* **101** 082402
[34] Li Z and Zhang S 2004 *Phys. Rev. Lett.* **92** 089402
[35] Kunz A 2006 *IEEE Transactions on Magnetics* **42** 3219
[36] Borie B, Kehlberger A, Wahrhusen J, Grimm H and Kläui 2017 *Phys. Rev. Appl.* **8** 024017
[37] Thiaville A, Nakatani Y, Miltat J, Suzuki Y 2005 *Europhys. Lett.* **69** 990
[38] He J, Li Z and Zhang S 2006 *J. Appl. Phys.* **99** 08G509
[39] Beach G, Tsoi M and Erskine J 2008 *J. Magn. Magnet. Mater.* **320** 1272
[40] Kläui M 2008 *J. Phys.: Condens. Matter* **20** 313001
[41] Al Bahri M 2020 *J. Magn. Magnet. Mater.* **515** 167293